

Direct Polymer Intercalation in Single Crystal Vermiculite

Shelly D. Burnside,^{†,‡} Hsien-Chang Wang,[§] and Emmanuel P. Giannelis^{*,†}

Department of Materials Science and Engineering, Cornell University,
Ithaca, New York 14853, and Exxon Chemical Company, Baytown, Texas 77520-5200

Received October 20, 1998. Revised Manuscript Received January 11, 1999

A lightly brominated isobutylene bromomethylstyrene copolymer was directly intercalated into a single crystal of organically modified vermiculite. Polymer intercalation was monitored by X-ray diffraction (XRD) and was confirmed by Rutherford backscattering spectroscopy (RBS). Atomic force microscopy (AFM) images of a cleaved polymer-intercalated crystal showed raised hemispheres on an otherwise flat background. Calculations show these hemispheres to consist of possible chain fractions or single and multiple chains, depending on the reaction time.

Introduction

Recently, a large number of research groups have realized the potential offered by polymer matrix nanocomposites, i.e., polymers reinforced on a molecular or nanoscale level.¹ Our group and others have focused on reinforcement with novel layered silicates, either in the pristine hydrophilic or exchanged organophilic state.² Two distinct nanocomposite nanostructures have been identified with layered silicates. *Exfoliated* or disordered hybrids retain little or no registry between the silicate layers, which are typically separated by as much as 5–15 nm. *Intercalated* hybrids, on the other hand, retain registry between the host layers, albeit with an expanded gallery height or distance between layers, which reflects the incorporation of polymer chains into the structure.

Exfoliated nanocomposites have become the focus of several efforts, since they exhibit greatly enhanced properties, including increased modulus, decreased

permeability, decreased solvent uptake, and increased thermal stability.^{2h–l} Intercalated hybrids, on the other hand, represent ideal systems for studying polymers in confined environments. Electrical conductivity, for example, of intercalated polymers has been previously studied for a wide variety of inorganic hosts.³ The dynamics of the intercalated polymer chains in layered hosts has also been explored using such techniques as nuclear magnetic resonance (NMR), differential scanning calorimetry (DSC), and thermally stimulated current (TSC) spectroscopy.⁴ Furthermore, early work demonstrated the ability to synthesize stereoregular polymers in the confining galleries of layered systems.⁵ Yet despite these studies, a complete picture has yet to emerge regarding the structure of intercalated polymer chains.

Since its conception in 1986, atomic force microscopy (AFM) and other scanning probe microscopy techniques have emerged as nondestructive methods that yield topological information not easily accessible by more traditional microscopies.⁶ AFM is conducive to measuring soft samples, including biological and organic materials. Novel work has captured the temporal evolution of biological processes, including DNA adsorbing on mica and live human platelets developing and clotting.⁷

[†] Cornell University.

[‡] Current address: Laboratory of Photonics and Interfaces, Ecole Polytechnique Federale de Lausanne, 1015 Lausanne, Switzerland.

[§] Exxon Chemical Co.

(1) (a) For example: *Chem. Mater.* **1996**, *8*, Issue 8. (b) Jose-Yacamán, J.; Rendon, L.; Arenas, J.; Puche, M. C. S. *Science* **1996**, *273*, 223. (c) Landry, C. J. T.; Coltrain, B. K.; Landry, M. R.; Fitzgerald, J. J.; Long, V. K. *Macromolecules* **1993**, *26*, 3702. (d) Wen, J.; Wilkes, G. L. *Chem. Mater.* **1996**, *8*, 1667. (e) Messersmith, P. B.; Stupp, S. I. *Chem. Mater.* **1995**, *7*, 454. (f) Calvert, P.; Rieke, P. *Chem. Mater.* **1996**, *8*, 1715.

(2) (a) Giannelis, E. P. *Adv. Mater.* **1996**, *8*, 29. (b) Okada, A.; Kawasumi, M.; Usuki, A.; Kojima, Y.; Kurauchi, T.; Kamigaito, O. *Mater. Res. Soc. Symp. Proc.* **1990**, *171*, 45. (c) Okada, A.; Kawasumi, M.; Kurauchi, T.; Kamigaito, O. *Polym. Prepr.* **1987**, *28*, 447. (d) Usuki, A.; Kojima, Y.; Kawasumi, M.; Okada, A.; Fukushima, T.; Kurauchi, T.; Kamigaito, O. *J. Mater. Res.* **1993**, *8*, 1179. (e) Yano, K.; Usuki, A.; Okada, A.; Kurauchi, T.; Kamigaito, O. *J. Polym. Sci.: Part A* **1993**, *31*, 2493. (f) Kojima, Y.; Fukumori, K.; Usuki, A.; Okada, A.; Kurauchi, T. *J. Mater. Sci. Lett.* **1993**, *12*, 889. (g) Yano, K.; Usuki, A.; Okada, A.; Kurauchi, T. *Polym. Prepr. Am. Chem. Soc. Div. Polym. Chem.* **1991**, *32*, 889. (h) Messersmith, P. B.; Giannelis, E. P. *J. Polym. Sci. A Polym. Chem.* **1995**, *33*, 1047. (i) Messersmith, P. B.; Giannelis, E. P. *Chem. Mater.* **1994**, *6*, 1719. (j) Burnside, S. D.; Giannelis, E. P. *Chem. Mater.* **1995**, *7*, 1597. (k) Lan, T.; Pinnavaia, T. J. *Chem. Mater.* **1994**, *6*, 2216. (l) Lan, T.; Kaviratna, P. D.; Pinnavaia, T. J. *Chem. Mater.* **1995**, *7*, 2144. (m) Hutchison, J. C.; Bissessur, R.; Shriver, D. F. *Chem. Mater.* **1996**, *8*, 1597. (n) Wu, J.; Lerner M. M. *Chem. Mater.* **1993**, *5*, 835.

(3) (a) Mehotra, V.; Giannelis, E. P. *Solid State Commun.* **1991**, *77*, 155. (b) Mehotra, V.; Giannelis, E. *Solid State Ionics* **1992**, *51*, 1–8. (c) Kanatzidis, M. G.; Bissessur, R.; DeGroot, D. C.; Schindler, J. L.; Kannewurf, C. R. *Chem. Mater.* **1993**, *5*, 595. (d) Wang, L.; Schindler, J.; Thomas, J. A.; Kannewurf, C. R.; Kanatzidis, M. G. *Chem. Mater.* **1995**, *7*, 1753.

(4) (a) Wong, S.; Vasudevan, S.; Vaia, R. A.; Giannelis, E. P.; Zax, D. *J. Am. Chem. Soc.* **1995**, *117*, 7568. (b) Vaia, R. A.; Sauer, B. B.; Tse, O. K.; Giannelis, E. P.; *J. Polym. Sci. B Polym. Phys.* **1997**, *35*, 59. (c) Krishnamoorti, R.; Vaia, R. A.; Giannelis, E. P. *Chem. Mater.* **1996**, *8*, 1728.

(5) (a) Glavati, O. L.; Polak, L. S. *Neftekhimiya* **1964**, *4*, 77. (b) Glavati, O. L.; Polak, L. S.; Shchekin, V. V. *Neftekhimiya* **1963**, *3*, 905.

(6) Binnig, G.; Quate, C. F.; Gerber, C. *Phys. Rev. Lett.* **1986**, *56*, 930.

(7) (a) Thomson, N. H.; Kasas, S.; Smith, B.; Hansma, H. G.; Hansma, P. K.; *Langmuir* **1996**, *12*, 5905. (b) Radmacher, M.; Tillmann, R. W.; Fritz, M.; Gaub, H. E.; *Science* **1992**, *257*, 1900. (c) Drake, B.; Prater, C. B.; Weisenhorn, A. L.; Gould, S. A. C.; Albrecht, T. R.; Quate, C. F.; Cannell, D. S.; Hansma, H. G.; Hansma, P. K. *Science* **1989**, *243*, 1586.

On the atomic scale, two-dimensional periodic patterns formed by multilayer Langmuir–Blodgett films have been imaged.⁸ Single crystals of organic compounds such as tetracene have also been imaged, with AFM-derived crystallographic unit cells corresponding closely to those determined from X-ray crystallography.⁹

Additionally, scanning probe microscopies have yielded valuable information about polymeric thin films and surfaces. Surface tension values for poly(vinylpyridine) (PVP) were measured by applying Young's equation to AFM-imaged islands of PVP on polystyrene.¹⁰ Polystyrene films adsorbed on graphite, mica, or silicon substrates were observed to form islands composed of single chains or chain agglomerates.¹¹ Ethylene–propylene copolymers have also been grafted onto mica, forming elongated islands with width-to-height ratios of 8:1.¹² Furthermore, scanning tunneling microscopy (STM) has been used to show epitaxial growth of nylon 6 on a graphite substrate.¹³

Studies of inorganic materials have also benefited from the use of these new microscopy techniques. The surface of mica was one of the first substrates to be imaged with AFM on the atomic scale.¹⁴ Layered silicates, including montmorillonite, illite, and vermiculite, display regular atomic-scale patterns after ion-exchange with inorganic cations.¹⁵ Similarly, the surfaces of hydrotalcite, a layered double hydroxide, exhibit regular patterns on the atomic level following exchange with an organic acid.¹⁶ In addition to imaging ion-exchanged surfaces, AFM has been suggested to be an ideal technique for imaging intercalates in layered materials.^{15a} For example, increased separation between the SiO₄ tetrahedra in pillared montmorillonites has been suggested from AFM images.¹⁷ Monomolecular intercalates (potassium, pyridinium, and tetramethylammonium cations) in manganese hexathiohypodiphosphate, a layered inorganic material, were also imaged.¹⁸

In this paper we report the first direct polymer intercalation in single crystals of vermiculite using a brominated isobutylene bromomethylstyrene copolymer. Vermiculite, like the better known montmorillonite, belongs to the general family of 2:1 layered silicates. Previous efforts on polymer intercalation have used

exclusively polycrystalline powder samples with a particle size of a few microns rather than well-defined single crystals. The Br groups provide the favorable interactions with the organosilicate host required for intercalation. In addition, because of the low T_g (–65 °C), the polymer chains even at room temperature are already well into the melt and possess significant mobility, avoiding the higher intercalation temperatures required for glassy polymers (i.e., polystyrene). Intercalation of the polymer was confirmed by X-ray diffraction and Rutherford backscattering spectroscopy. AFM images of cleaved polymer intercalated crystals provide further evidence for the intercalation of the polymer and show islands corresponding to chain fractions or single and multiple chains for shorter and longer intercalation times, respectively.

Experimental Section

Materials. Llano vermiculite with an idealized unit cell formula of Mg[Mg₆](Si₆Al₂)O₂₀(OH)₄, corresponding to a cation exchange capacity of 2.6 mequiv/g, was obtained from the University of Missouri Clay Repository.¹⁹ Single crystals of approximately 0.5–1 mm × 0.5–1 mm × 0.5 mm were used. The inorganic cations in the vermiculite crystals were first ion-exchanged with lithium as follows: vermiculite crystals (1 g) were refluxed in about 200 mL of an aqueous solution containing 3 times the stoichiometric amount of LiCl (Aldrich) (0.30 g) for 4 weeks, and the solution was changed weekly. At the end of the reaction, the crystals were washed with distilled water. Between 5 and 10 drops of 1 × 10^{–3} M AgNO₃ were added to the filtrate. The formation of a precipitate signaled the presence of halide ions, and the crystals were washed until no precipitate was observed. The lithium-exchanged vermiculite crystals were then added to a roughly 200 mL aqueous bath, containing 1.6 g of dodecylamine (C₁₂H₂₅NH₂; Aldrich) and 7.5 mL of a 1 M hydrochloric acid solution (prepared by dissolving 8.3 mL of a concentrated hydrochloric acid solution (37 wt %, Fisher Scientific) in 100 mL of deionized water). The mixture of vermiculite and alkylammonium salt was allowed to age for 1 week at 60 °C. The crystals were repeatedly washed with hot ethanol and distilled water until no precipitate was detected when ≈10 drops of a 1 × 10^{–3} M silver nitrate was added to the wash solution.

The polymer, supplied by Exxon, is a random copolymer containing 97 mol % isobutylene, 2 mol % *p*-bromomethylstyrene, and 1 mol % *p*-methylstyrene. Molecular weight (M_w = 35 000; M_n = 20 000) was obtained by gel permeation chromatography (GPC) (Waters 486 equipped with a UV detector) on polystyrene standards) and corrected using the Mark–Houwink equation.

The organically exchanged crystals were immersed in a polymer bath under vacuum at 85 °C for periods of up to 21 days. GPC traces of the polymer bath before and after intercalation showed the same MW and polydispersity, suggesting that no significant polymer degradation or fractionation takes place.

Characterization. The vermiculite gallery height was monitored using a Scintag X-ray diffractometer with Cu K α radiation. Infrared analysis was performed using a Galaxy 2020 Fourier transform infrared (FTIR) spectrometer with a resolution of 4 cm^{–1}. Exchanged vermiculite crystals (20 mg) were combined with 200 mg of potassium bromide (Aldrich) in a mortar and pestle and ground. The resultant powder was pressed into a pellet and analyzed. The conformations of the alkylammonium cations were probed by analyzing the symmetric, ν_s , and asymmetric, ν_{as} , stretching vibrations using zero-point determination of the first derivative. A Nanoscope II atomic force microscope in contact mode was used for

(8) Schwartz, D. K.; Garnæs, J.; Viswanathan, R.; Zasadzinski, J. A. N. *Science* **1992**, *257*, 508.

(9) Overney, R. M.; Howald, L.; Frommer, J.; Meyer, E.; Guntherodt, H.-J. *J. Chem. Phys.* **1991**, *94*, 8441.

(10) Vitt, E.; Shull, K. R. *Macromolecules* **1995**, *28*, 6349.

(11) (a) O'Shea, S. J.; Welland, M. E.; Rayment, T. *Langmuir* **1993**, *9*, 1826. (b) Stange, T. G.; Mathew, R.; Evans, D. F. *Langmuir* **1992**, *8*, 920. (c) Zhang, L. S.; Manke, C. W.; Ng, K. Y. S. *Macromolecules* **1995**, *28*, 7386. (d) Shelden, R. A.; Meier, L. P.; Caseri, W. R.; Suter, U. W.; Hermann, R.; Mueller, M.; Hegner, M.; Wagner, P. *Polymer* **1994**, *35*, 1571.

(12) Yang, J.; Laurion, T.; Jao, T.-C.; Fendler, J. H. *J. Phys. Chem.* **1994**, *98*, 9391.

(13) Sano, M.; Sasaki, D. Y.; Kunitake, T. *Science* **1992**, *258*, 441.

(14) For example, Erlandsson, R.; Hadziioannou, G.; Mate, C. M.; McClelland, G. M.; Chiang, S. *J. Chem. Phys.* **1988**, *89*, 5190.

(15) (a) Hartman, H.; Sposito, G.; Yang, A.; S. Manne, S. A.; Hansma, H. G.; Hansma, P. K. *Clays Clay Miner.* **1990**, *38*, 337. (b) Garnæs, J.; Lindgreen, H.; Hansen, P. L.; Gould, S. A. C.; Hansma, P. K. *Ultramicroscopy* **1992**, *42–44*, 1428.

(16) Cai, H.; Hillier, A. C.; Franklin, K. R.; Nunn, C. C.; Ward, M. D.; *Science* **1994**, *266*, 1551.

(17) Occelli, M. L.; Drake, B.; Gould, S. A. C. *J. Catal.* **1993**, *142*, 337.

(18) (a) Lagadic, I.; Clement, R.; Kahn, O.; Ren, J.; Whangbo, M. H. *Chem. Mater.* **1994**, *6*, 1940. (b) Lagadic, I.; Clement, R. *Microsc. Microanal. Microstruct.* **1993**, *4*, 453.

(19) Johns, W. D.; Sen Gupta, P. K. *Am. Mineralogist* **1967**, *52*, 1706.

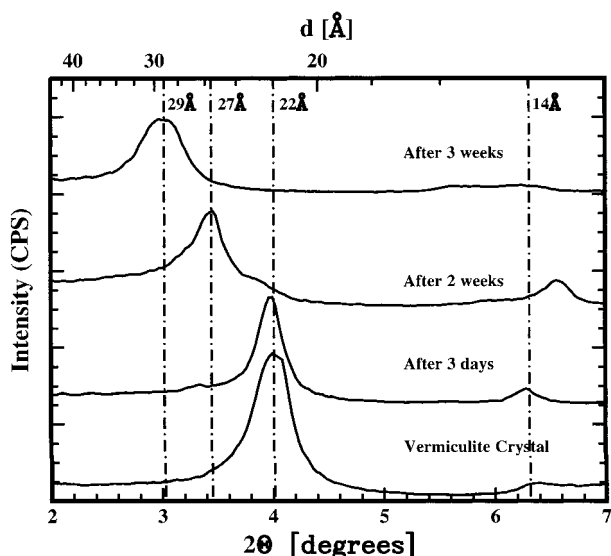


Figure 1. X-ray diffraction patterns showing the temporal evolution of a dodecylammonium vermiculite crystal reacted with a lightly brominated isobutylene *p*-methylstyrene copolymer.

imaging at a scan rate of 7–12 Hz with silicon nitride tips (force constant 0.1 N/m). Vermiculite crystals were cleaved prior to imaging, exposing a clean surface for analysis. Bromine content was analyzed using Rutherford backscattering spectroscopy (RBS). Details of the instrument used and the analysis have been given elsewhere.²⁰ Prior to RBS analysis, the vermiculite sample was cleaved and the edges trimmed to prevent detection of any nonintercalated remnants of the polymer bath. As an additional precaution, the RBS beam was restricted to allow signal from only the central portion of the crystal.

Results and Discussion

X-ray Diffraction. When the organically exchanged vermiculite crystal was placed in the brominated polymer melt for 3 days, X-ray diffraction showed peaks corresponding primarily to the original exchanged vermiculite crystal (2.2 nm plus higher order harmonics) and a weak peak at ~ 2.8 nm (Figure 1). After 2 weeks, a peak centered at 2.7 nm became the predominant peak, with shoulders originating from the original vermiculite crystal and an incipient peak at higher *d* spacings (2.9–3.0 nm). After 3 weeks, a broad peak at ~ 3.0 nm dominated the spectrum. A second-order harmonic of this peak can be observed in Figure 1 at approximately 1.5 nm. The increases in *d* spacing and, therefore, gallery height are suggestive of polymer intercalation into the silicate layers. No further increases in gallery height were observed with longer exposure to the polymer bath. Most spectra show remnants of unexchanged lithium vermiculite, with a spacing of 1.3 nm. The crystal suffered tremendous damage during the course of intercalation from expansion of the galleries in the relatively large crystal and by repeated cycling in the viscous polymer melt. In the X-ray diffraction patterns, this damage can be seen in the form of increased peak breadth as the reaction proceeds as well as diminishing peak intensity. In contrast to the brominated polymer, no intercalation was observed when the organically modified vermiculite

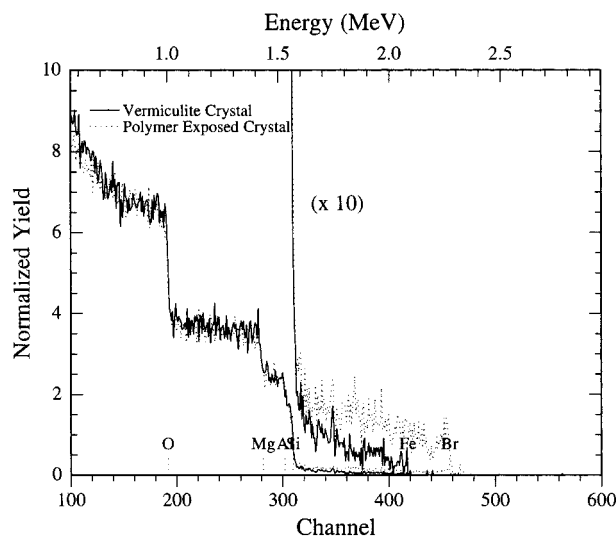


Figure 2. RBS traces from a dodecylammonium vermiculite crystal and a polymer reacted for 3 weeks with dodecylammonium vermiculite crystal. The region between channels 300 and 500 has been magnified 10 times to show the bromine content.

crystal was immersed in a nonbrominated polymer for periods of 21 days. Additionally, no intercalation was observed when a lithium-exchanged vermiculite crystal was immersed in the brominated polymer for the same time period.

Polymer chains typically intercalate into montmorillonite in a period of hours under static conditions.²¹ The extended period necessary for this experiment is consistent with the longer diffusional distances necessary for a millimeter-sized vermiculite crystal as compared to particles of montmorillonite or fluorohectorite with much smaller lateral dimensions (~ 1 – 5 μm). The experimental time is also in good agreement with an estimate obtained using the diffusion equation and a diffusion coefficient of 1×10^{-8} cm^2/s on the order of self-diffusion for a polymer of this molecular weight. This estimate is appropriate, as polystyrene chains intercalating into organically modified fluorohectorite show diffusion constants at least comparable to those of polymer chains in the melt.²¹

Rutherford Backscattering Spectroscopy. RBS is well-suited for detecting high *Z* (heavy) elements, such as bromine, in a matrix of low *Z* elements, as in the organically modified vermiculite crystal containing primarily silicon, oxygen, magnesium, and carbon. Both the polymer intercalated and unintercalated organically modified vermiculite show spectra characteristic of vermiculite (Figure 2). Analysis of the spectrum corresponding to the organically exchanged vermiculite crystal gave a stoichiometry of 3:3:1 Mg:Si:Al, in good agreement with literature values for Llano vermiculite ($\text{Mg}_3(\text{Si}_3\text{Al})\text{O}_{10}(\text{OH})_2$).²² In contrast to that of the unintercalated crystal, the RBS spectrum of the vermiculite exposed to the polymer shows also the presence of bromine, with a constant concentration through the crystal thickness analyzed (~ 10 μm). The crystal,

(21) Vaia, R. A.; Jandt, K. D.; Kramer, E. J.; Giannelis, E. P. *Macromolecules* **1995**, *28*, 8080.

(22) Brindley, G. W.; Brown, G. *Crystal Structures of Clay Minerals and Their X-ray Identification*; Mineralogical Society: London, 1980; Vol. 5.

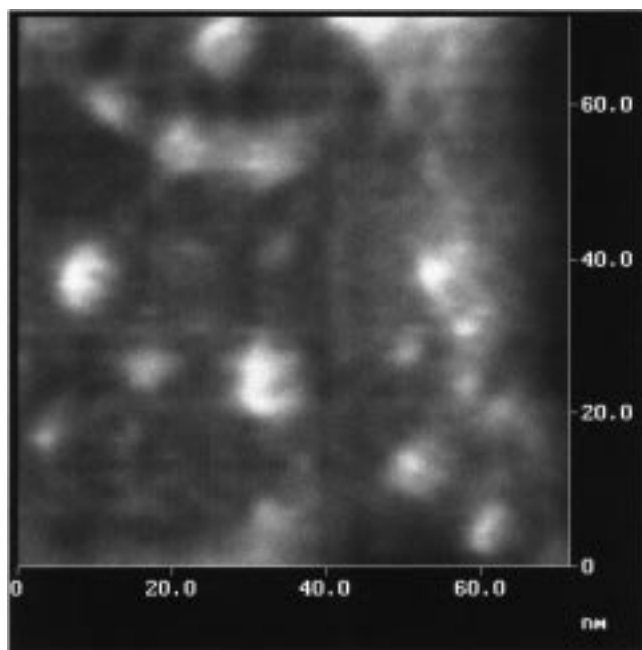


Figure 3. AFM image of organically modified vermiculite crystal reacted with the brominated copolymer for two weeks and then cleaved. White areas are approximately 0.3 nm above the black background. Refer to Table 1 for the dimensions of the features.

reacted for 2 weeks, showed between 0.7 and 1.8 Br atom/150 vermiculite $O_{10}(OH)_2$ formula units. In the crystal reacted for 3 weeks, the bromine concentration was calculated to be between 1.6 and 2.1 Br atoms per 150 vermiculite formula units. The large uncertainty arises from the broad RBS line width in combination with the small amounts of bromine in the polymer and precludes a statistically significant RBS analysis of the samples. Nevertheless, the presence of bromine with a constant concentration through the thickness of the sample does signal polymer intercalation, which is important for the AFM analysis presented in the following section. In addition, the amount of bromine increases for longer reaction times, suggesting that more polymer chains are intercalated, in agreement with the increases in gallery height. For further calculations the bromine concentration was taken to be an average of 1.8 Br atoms/150 structural $O_{10}(OH)_2$ units for the sample reacted for 3 weeks. Using the increase in gallery height and the crystallographically derived unit cell dimensions for vermiculite (0.5 and 0.9 nm),²² an experimental density of the polyisobutylene copolymer is calculated and is approximately 0.95 g/mL. This compares favorably with the literature value of 0.93 g/mL for pure polyisobutylene (PIB), especially as this value does not take into account the bromine on the copolymer used here.²³ The control experiments and the RBS analysis corroborate that the increased gallery height observed using X-ray diffraction corresponds to intercalation by the bromine-modified polymer.

Atomic Force Microscopy. Crystals which showed gallery height increases of 0.4 and 0.7–0.8 nm, reacted for two and three weeks, respectively, were cleaved and imaged in air using AFM. Typical images obtained are

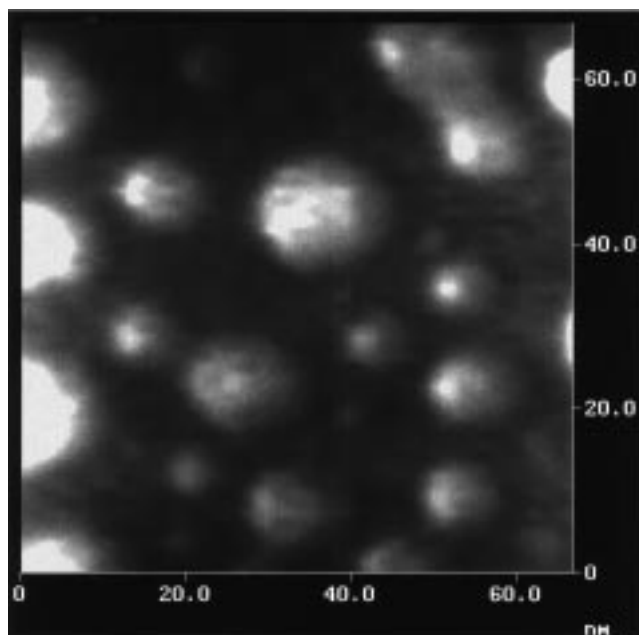


Figure 4. AFM image of organically modified vermiculite crystal reacted with the brominated copolymer for three weeks and then cleaved. Refer to Table 1 for the dimensions of the features.

Table 1. Dimensions of Polymer Hemispheres in AFM Images^a

system	width (nm)	height (nm)	volume ^b (nm ³)
polymer intercalated in vermiculite after 2 weeks	6 ± 2	0.3 ± 0.1	6
polymer intercalated in vermiculite after 3.5 weeks	11 ± 1.8	0.7 ± 0.2	44
	26 ± 8	1.5 ± 0.4	530

^a Each value represents the statistical analysis of 30–40 measurements. ^b Volume calculated as half-ellipsoid [$(1/2)(4/3)\pi(\text{width}/2)^2(\text{height})$].

shown in Figures 3 and 4. The widths and heights of the observed “bumps” or raised hemispheres are summarized in Table 1. Images did not vary by changing either the force or the scan rate. In addition, the images rotated upon rotating the samples, suggesting that they were not artifacts of the scanning conditions. As a control, an organically modified vermiculite crystal was also cleaved and imaged before polymer intercalation and did not consistently display any raised areas. The islands which were observed in one of six regions of the vermiculite crystal imaged are attributed to excess alkylammonium on the crystal surface, which is present either from the synthesis procedure or as a result of rearrangement during cleavage. Occasional extraneous small bumps have been previously observed in films of grafted organic polymers and have been attributed to excess organic material.²⁴ These impurities can be removed easily by washing the polymer surface.

Using geometrical considerations, we can calculate the volume of the features (islands) observed in the AFM images (Table 1).²⁵ For comparison, a single polymer chain of $M_n = 20\,000$ will occupy a volume of 35 nm³, assuming the density of the intercalated brominated polymer is equal to that of polyisobutylene. From the

(23) Brandrup, J.; Immergut, E. H. *Polymer Handbook*; John Wiley and Sons: New York, 1989.

(24) Zhao, W.; Krausch, G.; Rafailovich, M. H.; Sokolov, J. *Macromolecules* **1994**, *27*, 2933.

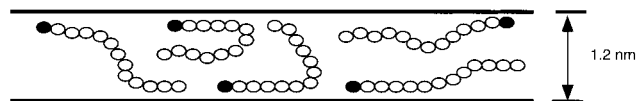


Figure 5. Idealized structure of a vermiculite crystal exchanged with primary dodecylammonium cations. Open circles represent CH_2 or CH_3 groups and filled circles the NH_3^+ groups. The surfactant chains are organized in a nominal trilayer.

RBS analysis, this assumption is fully justified. In the 2 week sample, the observed islands have a volume of 6 nm^3 , roughly one-sixth of the volume occupied by a single polymer chain. In the 3 week sample, we observe a bimodal distribution (Figure 4) and the raised half-ellipsoids have a volume of 40 nm^3 or 530 nm^3 , corresponding respectively to about 1 and 15 chains.

We present the schematics in Figures 5–7 as a representation of the processes occurring during intercalation and cleaving of the vermiculite crystal. Traditionally it has been suggested from the X-ray gallery height of 1.23 nm that the dodecylammonium chains in the vermiculite crystal form a tilted monolayer structure, with the chain forming an angle of 55° with respect to the surface, as calculated from the stretched chain length of 1.5 nm .²⁶ As vermiculite has a charge exchange capacity of 2.6 mequiv/g and crystallographically derived unit cell dimensions of 0.5 and 0.9 nm , there is approximately 0.2 nm^2 of interlayer area available per aliphatic chain, justifying the presence of extended chains with a cross sectional area of 0.18 nm^2 .²⁷ Recent work in our laboratory suggests, however, that the organic chains in the interlayer are not so well-ordered. The interlayer structure can be probed by monitoring the frequency of the CH_2 stretching and bending vibrations.²⁸ The organically exchanged vermiculite exhibits a $\nu_{\text{as}}(\text{CH}_2)$ infrared stretch of 2921 cm^{-1} , indicating that both gauche and trans CH_2 conformers coexist in the alkylammonium chains, implying a liquidlike environment for the surfactant chains. For comparison, the methylene chains in the all-trans ordered state of crystalline dioctadecyldimethylammonium bromide ($2\text{C}_{18}\text{N}^+2\text{C}_1\text{Br}^-$) exhibit a band at 2917.8 cm^{-1} . The band shifts to 2928.9 cm^{-1} when the chains are in a liquidlike environment, as in $2\text{C}_{18}\text{N}^+-2\text{C}_1\text{Br}^-/\text{CHCl}_3$ solution. Molecular dynamics simulations agree with the IR data showing surfactant chains packed in a trilayer with a random, liquidlike configuration, as shown schematically in Figure 5.²⁹

After polymer intercalation, the gallery expands first to 1.75 and then to 2.05 nm . The gallery height increases

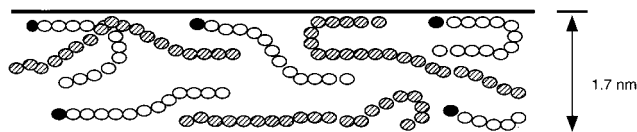


Figure 6. Idealized representation of a polymer-intercalated organically modified vermiculite. Open and filled circles are as in Figure 5 and correspond to the tethered surfactant. Chains with shaded circles correspond to the intercalated polymer. There is an increase of the gallery height upon intercalation with the chains in a four layer configuration.

correspond roughly to intercalation of one layer (0.4 nm) (Figure 6) and two layers (0.8 nm) of polymer, respectively. A mean-field model developed for polymer intercalation into organically modified layered silicates, supported by several experiments, suggests that polymer intercalation is driven by the presence of favorable interactions between the polymer and the host.³⁰ Experimentally, in the present study, the significance of these favorable interactions is verified by the failure of the nonbrominated, apolar polymer to intercalate into organically modified vermiculite.

According to this model, the driving force for polymer intercalation can be thought of as an interplay between the entropy and energy change in the system.³⁰ The entropic penalty of polymer confinement is compensated by the increased conformational freedom of the surfactant chains as the layers separate upon intercalation. However, the entropy change associated with the surfactant chains increases until the interlayer separation is equal to the fully extended length of the surfactant chains ($1-2 \text{ nm}$). On the other hand, as the interlayer separation increases, more polymer is confined and the total penalty of polymer confinement per unit area continuously increases. Therefore, the penalty for polymer confinement is compensated only up to a certain gallery height or interlayer separation, h_c . Since the total entropy change for gallery heights less than h_c is about zero, even relatively weak intermolecular interactions can provide the driving force for polymer intercalation. The amount of the intercalated polymer is, though, determined by the extent of the intermolecular interactions, as for gallery heights larger than h_c the penalty of polymer confinement dominates and strong energetic interactions are required to overcome the unfavorable entropy changes in the system.

We make three assumptions concerning cleaving of the vermiculite crystal to facilitate analysis of the AFM images. First, we assume the cations remain with the side of the crystal to which they were initially tethered, as necessitated by charge balance restrictions. We assume also no chain scission in either the polymer or the dodecylammonium chains, as the bond energy for C–C bond is 376 kJ/mol ,³¹ so the polymer ultimately will reside randomly with one or the other side of the crystal. Finally, we assume the polymer chain has sufficient energy to relax after the cleaving process, resulting in the spherical islands observed in Figures 3 and 4. Although we have no direct evidence of the structure of the polymer before cleaving, we suggest that

(25) We assume the islands are half-ellipsoids and calculate their volume from the dimensions measured by the AFM. A more accurate method which takes into consideration possible artifacts caused by the AFM tip (see, for example: Shelden, R. A.; et al. *Polymer* **1994**, *35*, 1571) has been described (Koutsos, V., Ph.D. Thesis, Groningen, The Netherlands, **1997**). The number of chains per island is calculated from the volume of the islands using the density and the molecular weight of the polymer.

(26) (a) Walker, G. F. *Clay Miner.* **1967**, *7*, 129. (b) Weiss, A. *Clays Clay Miner.* **1963**, *10*, 191.

(27) Lunden, B.-M. *Acta Crystallogr.* **1974**, *B30*, 1756.

(28) (a) Vaia, R. A.; Teukolsky, R. K.; Giannelis, E. P. *Chem. Mater.* **1994**, *6*, 1017. (b) Weers, J. G.; Sheuing, D. R. In *Fourier Transform Infrared Spectroscopy in Colloid and Interface Science*; Sheuing, D. R., Ed.; ACS Symposium Series 447; American Chemical Society: Washington, DC, 1991; Chapter 6.

(29) Hackett, E.; Manias, E.; Giannelis, E. P. *J. Chem. Phys.* **1998**, *108*, 7410.

(30) (a) Vaia, R. A.; Giannelis, E. P. *Macromolecules* **1997**, *30*, 7990. (b) Vaia, R. A.; Giannelis, E. P. *Macromolecules* **1997**, *30*, 8000.

(31) Ebbing, D. D. *General Chemistry*, 2nd ed.; Houghton Mifflin: Boston, 1987.

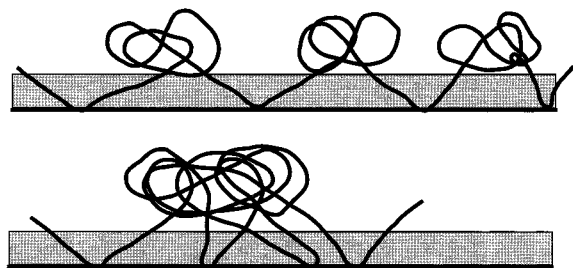


Figure 7. Schematic showing the surface of polymer-intercalated vermiculite crystal after cleaving as seen by the AFM: (a, top) 2 week sample and (b, bottom) 3 week sample. In the first the features correspond to a fraction of a chain while in the second to a whole chain. The alkylammonium chains are represented by the shaded area and are omitted for clarity.

the polymer is homogeneously distributed throughout the vermiculite crystal, as depicted in Figure 6, and that the observed islands are a consequence of relaxation and possible reorganization after cleaving due to the presence of the new polymer air interface (Figure 7).

The features in the two week sample with a volume approximately one-sixth of a single chain might correspond to segments or loops away from the silicate surface, which upon cleavage and the presence of the new polymer/air interface reorganize, forming approximately spherical caps (Figure 7a). Note that each polymer chain contains on average seven Br or anchoring sites as calculated from M_n and chemical formula and that the increase in gallery height upon polymer intercalation for the two week sample is similar to the height of islands observed in the AFM. Alternately, the islands might correspond to low molecular weight chains, which diffuse more rapidly through the vermiculite crystal. This latter explanation seems implausible, since both the molecular weight and the polydispersity of the polymer bath were the same before and after intercalation, suggesting that no significant fractionation has taken place. The three week sample shows a bimodal distribution with features corresponding to approximately one or multiple (fifteen) chains. GPC traces do not indicate a bimodal distribution in the polymer either, so these differences cannot be attributed to characteristics of the polymer. As more polymer chains intercalate inside the host layers and the gallery height increases, the amount of polymer per area increases. Upon cleavage, islands corresponding to one polymer chain are found (Figure 7b). Note that the gallery height increase is also similar to the observed islands for a single chain. We suggest that the ag-

glomerates of several chains are formed upon cleavage, as some of the polymer-tethering sites become loosened. These chains are free to join other chains, forming micelles, as previously observed in surface studies of styrene-vinylpyridine block copolymers grafted onto mica.³² The large agglomerates of multiple chains may be freer to follow the movements of the AFM tip as it sweeps over the bump, enlarging the measured height and width. Poly(ethylene oxide)/polystyrene (PEO/PS) copolymer chains grafted onto mica have been observed to migrate under the forces of the AFM tip.^{11a} To ascertain that all relaxation processes were concluded at the time of imaging, an intercalated vermiculite crystal was imaged both immediately and a week following cleavage after being stored at room temperature (well above the glass transition temperature for polyisobutylene) in a vacuum desiccator. The images were no different from those observed without aging, indicating that polymer relaxation, if it takes place, it does so rapidly.

Conclusions

The first direct intercalation of a polymer into single crystal vermiculite is reported. The importance of favorable intermolecular interactions in driving the reaction is demonstrated by the failure of the nonbrominated polymer to intercalate. Polymer intercalation is further supported by in-depth profiling using RBS. AFM images of an intercalated polymer are also reported by cleaving a vermiculite single crystal previously intercalated with the polymer. Removal of the wall causes rapid chain relaxation and possible reorganization into islands with volumes corresponding from a fraction of a chain to one and multiple chains (15) for shorter and longer intercalation times, respectively.

Acknowledgment. This work was supported in part by AFOSR. We would like to thank Dr. Richard Vaia for the organically exchanged vermiculite, Dr. Gerald Kraus and Dr. Jan Genzer for aid with the RBS and analysis, Dr. S. A. Haque for the lightly brominated polymer and GPC work, and Prof. Ramanan Krishnamoorti and Dr. Evangelos Manias for helpful insights. S.D.B. acknowledges the financial support of a DoD Fellowship. This study benefited from use of the NSF-funded Cornell Center for Materials Research facilities.

CM981026G

(32) (a) Stamouli, A.; Pelletier, E.; Koutsos, V.; van der Begte, E.; Hadziioannou, G. *Langmuir* **1996**, *12*, 3221. (b) Williams, D. R. M. *J. Phys. II* **1993**, *3*, 1313.